PHYSICAL REVIEW B VOLUME 18, NUMBER 7 1 OCTOBER 1978

A positron-lifetime study of irradiation effects in copper irradiated with energetic protons

Richard H. Howell
Lawrence Livermore Laboratory, Livermore, California 94550
(Received 18 January 1978)

Copper samples have been irradiated with protons in the energy range 4.5 to 25 MeV. The resulting damage effects in the copper have been studied with the positron-lifetime measurement. Evidence that the surviving defects are vacancylike is presented. The dependence of the defect production rate on proton energy and on irradiation temperature suggest that the defect production depends on more than one mechanism, one of which occurs only when the copper recoil energy is above a threshold of about 55 keV.

I. INTRODUCTION

The dependence of radiation effects on the energy distribution of the primary knock-on atoms (PKA) is a subject of current experimentation. As the energy of the recoiling atom increases, the nuclear scattering in the lattice decreases and a larger fraction of the energy is lost to electrons. This results in fewer defects. Experiments on silver irradiated at low temperature with protons tend to confirm the general trend of electronic losses based on the Lindhard theory for recoils above a few keV. However, defect-production efficiencies based on a modified Kinchin-Pease model are only 20% to 30%. At lower recoil energies the production efficiencies are near 100%.[1] The damage rates obtained at 40°K on Cu, Nb, and Pt with reactor neutrons and neutrons from 40-MeV D-Be reactions scale with integrated damage energy.[2] Similarly a comparison of reactor neutron, D-T fusion neutron, and 30-MeV D-Be neutron irradiations of Nb, V, and Mo also obtained damage rates which scale with damage energy.[3] Defect production efficiencies of 30% to 40% were obtained.

In a room-temperature experiment the mechanical effects produced in copper tensile specimens irradiated with neutrons has been shown to vary with the character of the neutron source.[4] Specimens irradiated by ~14 MeV neutrons produced by D-T fusion at the Lawrence Livermore Laboratory (LLL) Rotating Target Neutron Source (RTNS) showed an increased damage rate over speciments irradiated with fission neutrons from the Livermore pool-type reactor when normalized to displacements per atom. The energy spectra of the PKA produced by these two sources differ in distribution and endpoint energy, with that of the D-T fusion neutrons having higher endpoint and average energy values. Effects which are the result of PKA spectrum differences can better be studied by proton irradiation. The PKA spectra of energetic protons have been shown to closely resemble that of D-T neutrons[5] while that from low-energy protons shares many characteristics with that from fission neutrons. Comparisons of damage effects resulting from low- and high-energy proton irradiations should exhibit similar dependence on the PKA spectra as those neutron comparisons.

In the experiment reported here, proton irradiations are used at different proton energies, particle doses and irradiation temperatures to study the PKA energy dependence of surviving defect production in room-temperature irradiations. Positron lifetime measurements have been used to probe defect concentrations and identify defect characteristics. The dose dependence of the defect production was determined for particle doses to 10^{18} p/cm^2 at two proton energies, 20.5 and 4.5 MeV. Energy dependence in the range of 4.5–24 MeV and irradiation temperature dependence from −40 to 46°C were also measured. Isochronal annealing studies were performed on selected samples.

The data from the position lifetime measurements were analyzed with a single-trap model and experimental defect concentrations were calculated using published trapping rates for unit defect concentration. Analysis was attempted with a two-trap model, however, no evidence for a second trap was obtained. These are compared with calculated defect concentrations and defect production efficiencies are obtained respectively for two traps, vacancies and dislocations and two models for defect production. Evidence for a possible energy threshold in the PKA defect production is derived from these comparisons and a consistent identification of the trap as having the properties of a vacancy is obtained from these and other data.

II. DISPLACEMENT CALCULATIONS

Calculated values of defect production were used to establish the energy and dose ranges used in this experiment. The PKA energy spectrum for

protons bombarding copper is calculated using models borrowed from nuclear physics. These models include the experimental observation that the nonelastic fraction of the total scattering cross section increases as the proton energy increases, and is larger than the elastic cross section at the upper energies in this experiment. Recoil spectra from elastic scattering are calculated using the nuclear optical model which also provides total inelastic scattering strength. The nonelastic recoil energy distribution is then calculated by assuming the nucleus is left in a distribution of excited states characterized by a nuclear temperature. Details of this method and similar calculations may be found in Refs. 5 and 6. Having calculated the strength and energy distribution of the PKA, the damage energy distribution $E_D(T)$ may be obtained by multiplying each element in the energy spectrum by the fraction of the energy lost in nuclear scattering events in the slowing down of the recoiling atom and all successive generations of recoils. The fraction of the total energy available for nuclear scattering is calculated using the Lindhard theory.[7] The integral over recoil energy T of the damage energy spectrum from some threshold to the maximum recoil energy is the total damage energy cross section.

The integral of the damage energy weighted as below is the total displacement cross section $\sigma(D)$

$$\sigma(D) = \int_0^{T_{\max}} \nu(T) E_D(T) dT .$$

In the displacement model the factor $\nu(T)E_D(T)$ represents the number of Frankel pairs produced and is conventionally chosen to be

$$\nu(T)E_D(T) = \begin{cases} 0, & T < E_d \\ 1, & E_d < T < 2E_d \\ 0.8E_D(T)/2E_d, & 2E_d < T . \end{cases}$$

The energy E_d is the direction-averaged energy required to create a single lattice displacement; 32 eV for copper. A second model which may be used in situations involving energetic cascades is the threshold model for which

$$\nu(T)E_D(T) = \begin{cases} 0, & T < \text{threshold} \\ 0.8E_D(T)/2E_d, & T \geq \text{threshold} . \end{cases}$$

The threshold energy corresponds to the minimum PKA energy for which energetic cascades become the dominant feature in the damage production. This model may be applicable in the temperature regime in which single vacancies are mobile and only cascade damage remains.

Recoil energy distributions for protons on copper at 5-, 10-, 15-, 20-, and 25-MeV incident energies[8] are in Fig. 1. These spectra may be compared to one another and to neutron recoil spectra from the RTNS fusion neutron source[9] and from Experimental Breeder Reactor II (EBR II), row 7.[10] For the 5-MeV spectrum the distribution is simply that of Rutherford scattering. However, at higher energies, inelastic contributions and diffraction effects in the elastic contribution become evident. The reactor spectrum from EBR II produces very-low-energy recoils. That general feature is similar to the proton recoil spectrum from 5-MeV protons, and to the extent of that similarity, the same effects will be observed.

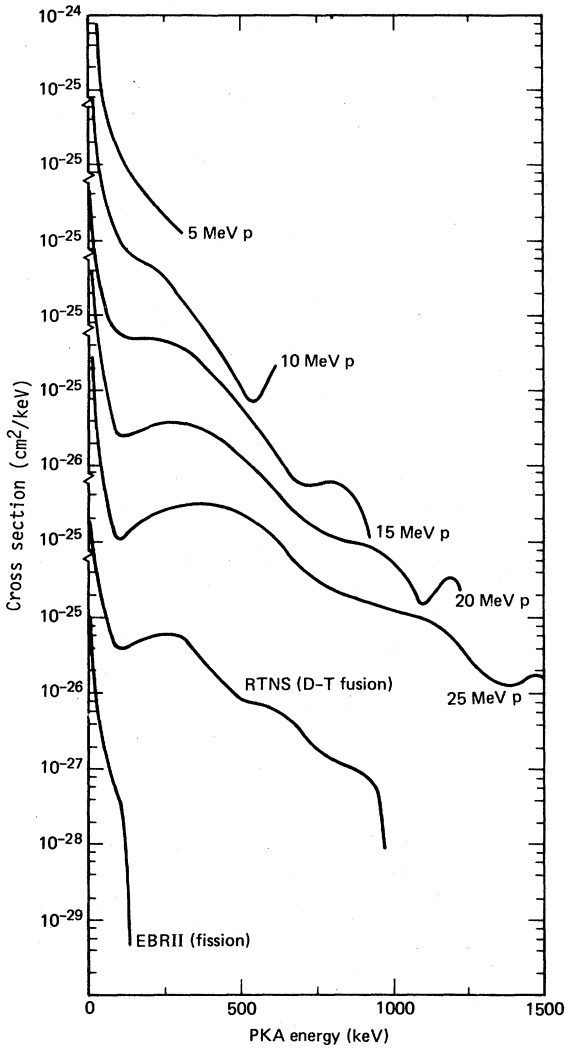

FIG. 1. Energy spectra for the primary knock-on atoms (PKA) produced in copper irradiated with protons as a function of proton energy. Note the offset in the intensity scale. Similar spectra from two available neutron sources, RTNS (D-T fusion) and EBRII (fission) are included for reference.

The recoil spectrum from ~14.5-MeV neutrons produced at RTNS, shares characteristics with the recoil spectrum produced with protons in the 15- to 20-MeV range. The main difference is that the neutron recoil spectrum has less strength in the very-low-energy recoil region than does the proton recoil spectrum.

III. EXPERIMENTAL METHOD

A. Positron measurement characteristics

There has been considerable evidence presented that positrons are trapped at defects in metals and exhibit changes in characteristic center-of-mass momenta and annihilation lifetime compared to free positrons. These changes which may be observed by measuring the lifetime, Doppler broadening, or angular correlation characteristics of the annihilation γ ray have been used to study vacancies in thermal equilibrium in several materials including copper,[11,12] and dislocations produced by cold work in copper.[13] Copper damaged by fission-reactor neutrons has been studied with the Doppler-broadening technique.[14,15] The recovery of copper damaged by energetic electrons has also been studied by Doppler broadening[16] and annihilation lifetime measurements.[17,18]

B. Positron lifetime spectrometer

Positron lifetime measurements have been used in this study to quantify the defect production in room-temperature proton irradiations. The annihilation radiation was detected in a coincidence spectrometer consisting of two 3.8-cm by 2.54-cm diameter cylinders of Pilot U mounted on RCA 8850 phototubes. Both Ortec 270 constant-fraction discriminators and Ortec 473A constant-fraction discriminators were used in the experiment at different times. Resolution in these systems measured with ^{60}Co varied from 280 to 310 psec for 50% pulse-height windows set in the working range for the positron measurement. The environment around the electronics and detectors was maintained at a constant temperature to within 0.5 °C. No external gain stabilization was used.

Positron sources were prepared by evaporating approximately 5 μCi of ^{22}Na on a 1-mg/cm^2-thick Ni foil which was then folded over, covering the radioactive area. The singles counting rates obtained with this source were 2×10^3 counts/sec. Because of the low singles rates, peak-to-background ratios were 15 000 to 1 in spectra taken with unirradiated samples. Source related contributions to the spectra obtained are 4% of the total coincidence counts above background. About 2×10^5 counts were collected in each spectrum during a typical 23-h run. Some of the irradiated samples measured in this experiment contained radioactive ^{65}Zn. In general this resulted in higher random background rates and required that the detectors be collimated for the most active samples, so scattering events from one detector to the other were minimized. Because ^{65}Zn γ rays are not correlated in time, the decay produces no direct contribution to the coincidence spectra.

C. Lifetime spectra analysis

Spectra were analyzed with a number of separate models including single lifetime and trapping models. The spectra were fit with the minimization subroutine ZXSSQ available from the International Mathematics Subroutine Library. The prompt response of the coincidence system was chosen to be the slope sided function of Ref. 19 which was found in this experiment to give an excellent description ($\chi^2/N \leq 1$), of a prompt spectrum obtained with ^{60}Co. Background and source contributions were included directly in the model calculation of the data. In the analysis of the data, fits were done obtaining either an average lifetime by forcing a single lifetime model to fit the data or trapping rates from a model which explicitly included the trapping rate and the free and trap lifetimes. Both models contain representative values for the parameters describing source and resolution characteristics. In general the only values which were not allowed to vary freely in the fit were: the lifetime of the source contribution, and in the trapping model, the free and trap lifetimes. In no case during the experiment did the strength of the source contribution vary significantly from 0.04 of the total strength.

Measurements of the radioactive decay of a 10-μCi source of ^{207}Bi were made to check the entire lifetime experiment. This source decays by β emission ($T_{1/2}=38$ years) to an excited state in ^{207}Pb which decays by emitting a 1064-keV γ ray to a metastable state at 569-keV excitation. The lifetime of the metastable state is measured to be 186 psec.[20] Thus this source serves as a simulation of the lifetime measurement with ^{22}Na and annealed metal samples. The value of the lifetime of the metastable state in lead measured in this experiment is 189 ± 5 psec in close agreement with the accepted value and as only one lifetime component was found in the analysis, this datum provided an additional check of the spectrometer electronics.

D. Sample preparation

Sample disks 1.9 cm in diameter and 0.305 mm thick of MRC Marz grade polycrystalline copper

were prepared by annealing at 650 °C for 2 h in a reducing atmosphere and then electropolishing to 0.252 ± 0.003 mm final thickness. Positron lifetime measurements on samples prepared in this manner show only one lifetime. This was used as the value of the free annihilation lifetime in the trapping model.

E. Sample irradiation and measurement

The samples were irradiated in stacks of four so that as the protons lost energy passing through the copper, each sample in the stack was damaged by protons of different energy. For each dose, two stacks of samples were irradiated so that in each case a positron source could be sandwiched between two samples in a symmetric manner. The incident proton energy was 24.00 ± 0.010 MeV with an energy spread of 0.015 MeV full width at half maximum (FWHM). The exiting proton beam is broadened by straggling to a Gaussian energy distribution with 1.5-MeV FWHM.[21]

The proton energy is decreasing as the proton beam passes through the stack of samples. Thus the recoil-spectrum characteristics, damage-energy cross section, and displacement per atom (DPA) rates are a function of the position of each sample in the stack and the depth in each sample. In Fig. 2, the proton energy and integrated damage-energy cross section are graphed as a function of position in the sample stack. The proton energy graphed is the average proton energy, and the integrated damage-energy cross section has been averaged over the proton-straggling energy distribution. Calculated average proton energies at the sample surfaces are 24, 20.5, 16.7, 11.5, and 4.5 MeV.[22]

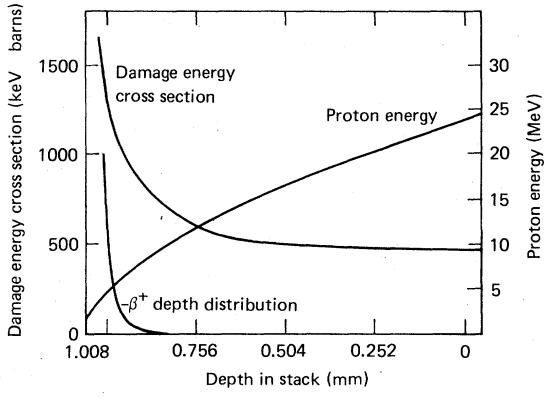

FIG. 2. Relationship between proton energy, damage energy and the depth of the copper sample in the sample stack. In the experiment, protons entered from the left with an initial energy of 24 MeV. As the proton penetrated the stack, energy was lost to electronic excitation so that the exiting proton had only 4.5-MeV energy. The integrated damage energy cross section is proportional to the DPA calculated in the displacement model. Also shown is the distribution of positrons in the last sample for the case of a positron source at the 4.5-MeV surface.

The proton beam was rastered over a 0.317 cm^2 circular collimator in front of the samples in order to ensure a spatially uniform dose over the irradiated area. The average current density was 3.2 $\mu A/cm^2$ during most runs. Heat deposited in the samples by the proton beam was removed through an alcohol-cooled brass heat sink in which the stack of samples was spring loaded. The outer diameter of each of the samples was in good contact with the heat sink, and the irradiated area of all samples was in mechanical contact with each other. The irradiated area of the last sample in the stack was in direct contact with the heat sink.

A calculation of the maximum variation between the temperature of the center of the sample and that of the heat sink may be made by considering the contact area of the sample holder. This maximum is 2.0 °C for the geometry and beam current in this experiment. The heat-sink temperature was held at −5 °C during most of the runs. An exception was made for those sets of irradiations used to study irradiation temperature dependence in which the temperature ranged from −40 to +46 °C. The samples were held at these temperatures only during the irradiations. They were allowed to warm to ambient temperatures directly following the run. Measurements of the damage followed weeks later.

Sample dosimetry was done by integrating the charge deposited in the heat sink behind the samples. These values were confirmed by measuring the radioactive decay of ^{65}Zn at a later date.

IV. RESULTS

The response of a positron measurement is an average of the sample characteristic over the range of the positrons in the sample, weighted by the positron distribution. For a ^{22}Na source sandwiched between copper samples, this depth distribution is exponentially decreasing with a constant of 23.1 μm.[23] Consequently, the positron measurement is heavily weighted to conditions near the surface of the samples providing two sets of data from each sample set, one for each surface.

Average lifetime data as a function of proton dose are shown in Fig. 3 for two separate proton energies. The lower-energy data were obtained from the low-energy side of the last sample in the stack, $\bar{E}$ ~4.5 MeV. The higher-energy data were

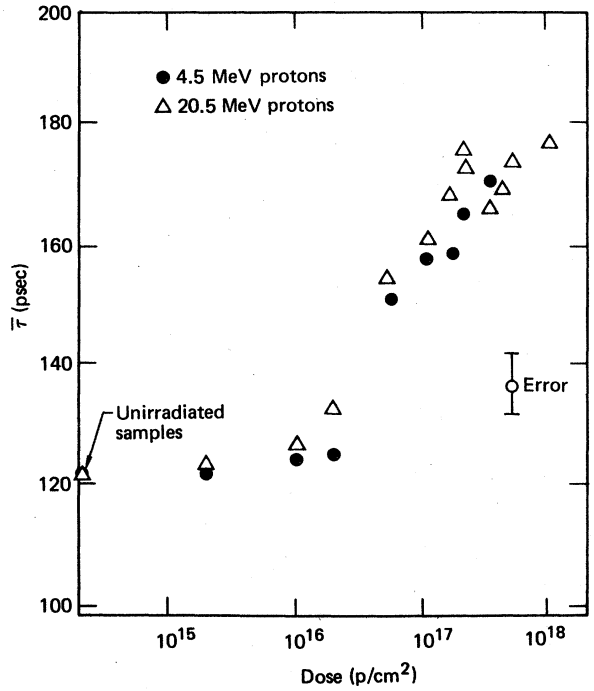

FIG. 3. Average lifetimes of positrons in proton irradiated samples as a function of proton dose. The highest dose values are in saturation for both the low- and high-energy irradiations. The temperature of irradiation for all these samples was -4 °C. The error represents a statistical error obtained from analysis of repeated measurements of annealed copper samples.

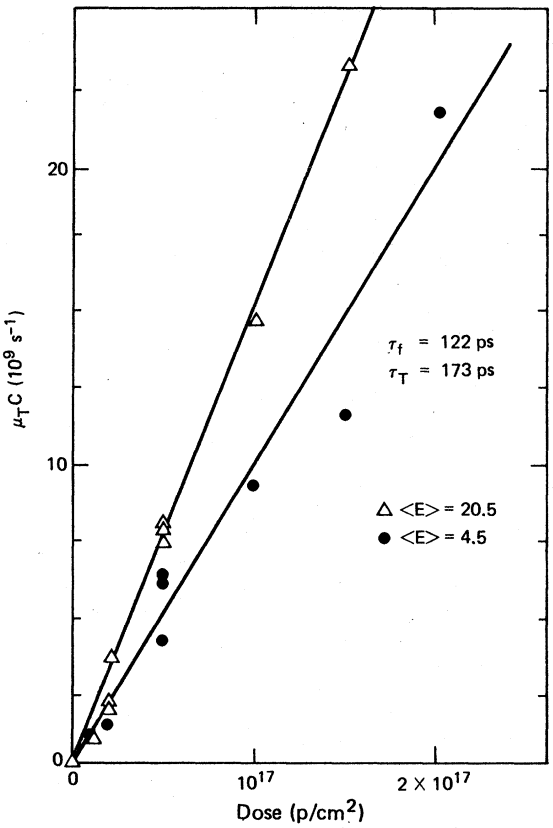

FIG. 4. Trapping-rate values ($\mu_T C$) for two energies as a function of proton dose. The energies of the samples refer to the energies of the protons in the surface nearest the positron source during measurement. In both samples, the positron source was sandwiched between the low-energy side of the samples. The lifetime values used in the single-trap model were 122 psec for the bulk lifetime and 173 psec for the lifetime of the trap. The dose dependence of the trapping rate is linear to a high degree. Least-squares fits of the slope give values of 1.48×10^{-7} sec^{-1} proton^{-1} cm^2 for the high-energy samples and 0.96×10^{-7} sec^{-1} proton^{-1} cm^2 for the low-energy samples. Values of the trapping rate significantly above 2.5×10^{10} sec^{-1} cannot be obtained because of saturation in the positron measurement. An estimate of the reliability of the trapping rate values can be obtained from the standard deviation of the χ^2 distributions of the linear fits. These are 0.55×10^9 sec^{-1} for $E_p = 20.5$ MeV and 1.8×10^9 sec^{-1} for $E_p = 4.5$ MeV. The larger variance in the low-energy samples is probably due to variations in the proton straggling at the sample position induced by slight variations in sample thickness.

from the low-energy side of the first sample in the stack, $\bar{E} \sim 20.5$ MeV. The higher dose values are in saturation for both the low- and the high-energy irradiations. The value for the annealed lifetime is 122 ± 5 psec and the value for the saturated lifetime is 173 ± 5 psec. These values were used in the trapping-model analysis of the data and are in remarkably close agreement with values published for deformed copper.[24]

Using the annealed and saturated lifetimes, the data have been reduced in a single-trap model. The trapping-rate analysis is limited to doses less than saturation, as at saturation all positrons are trapped and the trapping rate is indefinite. The fits with a single-trap model are better than those with an average lifetime, particularly when the residual spectrum of the fit was examined. The average lifetime fits resulted in a residual spectrum with distinct oscillating structure while that from the trapping model was smooth and centered on zero within the statistics of the measurement. For a single trap model χ^2/N improved by about 40% ($\chi^2/N \sim 1$). No evidence for more than one trap could be found from the data analysis. A linear least-squares fit to the results of a single-trap analysis of the data is shown in Fig. 4. Values of the trapping rate ($\mu_T C$) per unit particle dose for both the 20.5-MeV irradiations and the 4.5-MeV irradiations obtained are 1.48×10^{-7} sec^{-1} proton^{-1} cm^2 for the 20.5-MeV irradiations and 0.96×10^{-7} sec^{-1} proton^{-1} cm^2 for the lower energy.

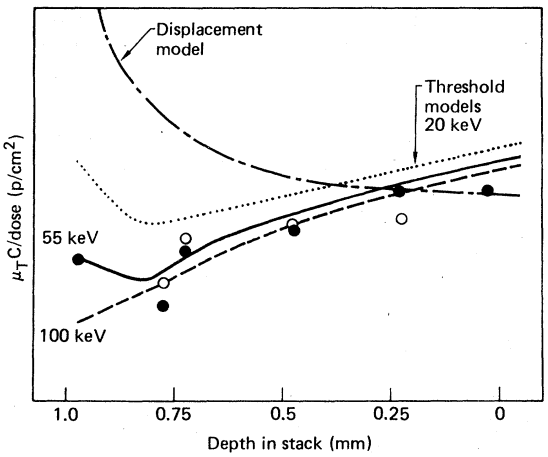

FIG. 5. Trapping rate ($\mu_T C$) per proton/cm^2 as a function of depth in the stack. Data are plotted at the average penetration depth of the positrons from the source. DPA calculations are shown for the displacment model and the threshold model. The displacement-model calculation and the threshold-model calculation at 55 keV have been normalized to the data at 20.5 MeV which is plotted at a depth of 0.23 mm. The dip in the threshold model at about 0.76 mm into the stack is seen in the data for two separate doses plotted with open and closed circles.

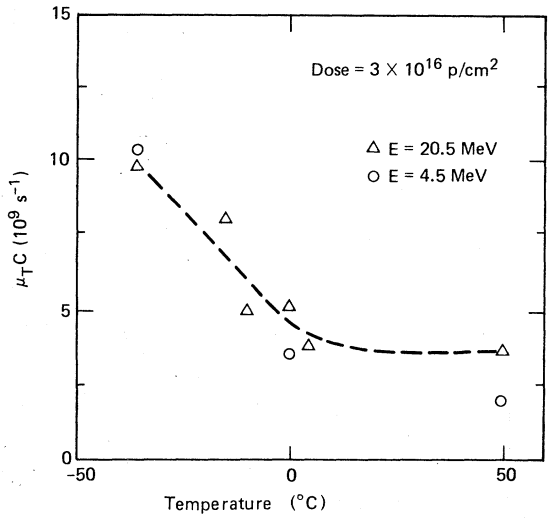

FIG. 6. Trapping rate ($\mu_T C$) as a function of irradiation temperature. The trapping rate for those samples which were irradiated at temperatures which froze in the damage produced by the lower-energy recoils is enhanced over the trapping rate per proton/cm^2 found in those samples which were irradiated at a higher temperature. The ratio of high- to low-energy irradiations is also affected by the change in the irradiation temperature.

The behavior of the positron lifetime as a function of proton energy at constant proton dose and constant temperature at the heat sink, has been determined by measuring successive samples in the stack. Each side of each sample was measured separately for those samples where the recoil characteristics were changing rapidly. Trapping-rate values were obtained for these data with a single-trap model. The trap and bulk material lifetimes were fixed to the same values as in the previous analysis. The results are presented in Fig. 5, in which values of the trapping rate per unit dose are plotted at the depth of average penetration of the positrons. There is a general decrease in the measured values as the proton energy changes from 24 to 4.5 MeV. The difference in trapping rate at the 11.5-MeV proton energy boundary in the high- and low-energy samples is repeatable in samples at two doses.

In Fig. 6 are plotted the results of analysis of samples which were irradiated at several temperatures for doses near 3×10^{16} p/cm^2. Small corrections of less than 10% were made to some of the trapping rate values by assuming that the trapping rate varied linearly with total particle fluence and adjusting the trapping rate value by the ratio of the experimental value to the reference dose. The irradiation geometry and lifetime measurement geometry are the same as those samples previously analyzed and labeled by the energies 4.5 and 20.5 MeV. The trapping-rate analysis was done with the same values for lifetimes as used in the previous analysis. To check the trap lifetime, analysis of this data set was also done leaving the trapped lifetime as a parameter of the fit. Values of the lifetime obtained were near that chosen in the previous fits. However, the scatter in the trapping rate values was increased by this analysis method and the results are not presented here.

The overall stability of the traps can most easily be determined by isochronal annealing studies. Two such studies were done on samples which were irradiated at −4 °C; one on a sample set irradiated at 20.5 MeV to a dose of 2×10^{17} p/cm^2, the second on a sample irradiated at 4.5 MeV to a dose level of 5×10^{16} p/cm^2. The annealing at all temperatures was done for 30 min in a reducing atmosphere after which positron measurements were done at room temperature. In the low-dose sample the initial value of the average lifetime was intermediate to the annealed and the saturated lifetime while the higher-dose sample was at saturation. The results of the annealing studies are presented in Fig. 7. Only an analysis of the average lifetime is presented, as there is no definition of the value of the trapping rate in a saturated sample.

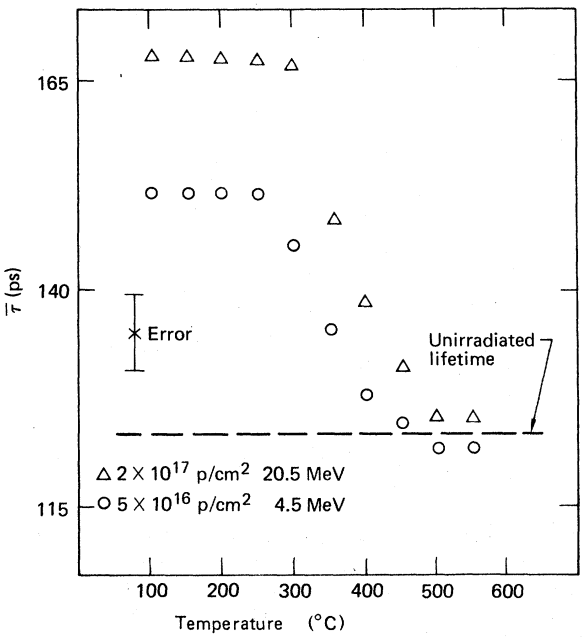

FIG. 7. Average lifetime as a function of annealing temperature for two samples. The triangles are a sample irradiated to a dose of 2×10^{17} proton/cm^2 and measured at 20.5-MeV geometry used in the measurements shown in Fig. 3. The sample lifetime was in saturation at the beginning of the anneal sequence. The dots are a sample irradiated to 5×10^{16} proton/cm^2, and measured in the geometry of the 4.5-MeV measurements in Fig. 3. The temperature at which the damage characteristics begin to change is typical of either vacancy groups of dislocations.

V. DISCUSSION

In the average-lifetime analysis of the positron data in Fig. 3, the value for the saturated lifetime is the same for the samples irradiated with high- and low-energy protons. This suggests that the surviving defect is of the same character for both the high- and low-energy irradiations. The value of the saturated lifetime is typical of those values measured for monovacancies formed thermally or by electron irradiation.[17,18] The lifetime of positrons trapped at vacancies produced by low-temperature electron scattering is 180 ± 10 psec which is in agreement with the value used here of 173 ± 5 psec. It has been suggested that the stable defects observed in copper from irradiation at room temperature with neutrons are dislocations.[14,15] The measured lifetime change for dislocations in copper is 34 psec.[25] The lifetime change observed for dislocations is not enough to produce the saturated lifetime value observed here. Most likely, the dominant defect type is vacancylike.

When the positron lifetime data are analyzed in terms of a single-trap model, the total trapping rate is seen to vary linearly with dose for both the high- and low-energy irradiations. The slope is proportional to the trap-production rate per proton. These rates may be compared to defect calculations at separate irradiation energies. The ratio of the defect-production rate in the high-energy irradiation to the defect-production rate in the low-energy irradiation is measured to be 1.5. However, displacement model damage rates averaged over the damage distribution and weighted by the distribution of positrons in the sample, predict the ratio to be 0.4 ± 0.02. Clearly the surviving defect rate measured in this experiment is not well scaled by calculations in the displacement model for which the rate of surviving defects is 3.8 times lower.

The relative values of the trapping rate can be compared directly among samples as a function of dose or energy. If one knew the identity of the trap and the trapping rate for an individual trap, (μ_T), then the concentration of traps (C) could be extracted from these data as well. Individual trapping rates for two particular defects, dislocations and vacancies, are available from previous experiments. The trapping rate for dislocations introduced by cold work has been measured to be $(2.9\pm1.0)\times10^{15}$ sec^{-1}.[25] The trapping rate for vacancies has been deduced in Ref. 13 from measurements in Ref. 12 to be 2.5×10^{14} sec^{-1}. There is sufficient difference between these two rates to suggest that the rates are distinct and that a comparison of the defect concentration determined by trapping-rate data and that calculated with the displacement and threshold models is informative.

Using the values for the trapping rate per defect for each defect, the surviving concentration of (displacements/atom)/(proton/cm^2) is obtained. This value is comparable to the calculated DPA values in the displacement model or threshold model. The values for these rates and the efficiency of defect survival are presented for each energy and model in Table I. The most positive indication that may be drawn from the values in Table I is that the defects are probably not dislocations. This conclusion also drawn from the values of the saturated lifetimes is supported by the comparison of the defect concentration at high energies with either model for calculating DPA. A survival efficiency of more than 20% must be obtained to be consistent with those values obtained in other experiments where survival efficiencies of 20% to 40% have been obtained.[1-3] The low values obtained for dislocations along with the value for the saturated lifetime, suggest that the defect is vacancylike. The values of survival efficiency,

TABLE I. Trapping rate per unit dose and the resulting defect concentrations per unit dose are compared with calculated damage rates for two models. The survival efficiency values suggest that the positron traps may be vacancylike. For a full explanation of the values presented here, see text.

E_p (MeV)	$\mu_T C$ (10^7 sec^{-1} proton^{-1} cm^2)	Dislocation production (cm/cm^3) proton^{-1} cm^2	Calculated DPA rate DPA proton^{-1} cm^2	(model)	Survival efficiency Displacements (R_0 = 20 Å) (DPA in loop)/DPA	Dislocations (cm/cm^3)/DPA
20.5	1.48	4.9×10^{-23}	6×10^{-21}	(displacement)	0.04	0.008
20.5	1.48	4.9×10^{-23}	3.25×10^{-21}	(55-keV threshold)	0.07	0.015
4.5	0.96	3.2×10^{-23}	1.4×10^{-20}	(displacement)	0.01	0.002
4.5	0.96	3.2×10^{-23}	2.12×10^{-21}	(55-keV threshold)	0.07	0.015

obtained by assuming the defects are dislocations, cannot be used to completely rule out this defect type. The number of displacements which form a loop determine the loop area, however, the efficiencies obtained are in units of length of the edge of the loop per unit material volume so that there is some average loop size which will result if the efficiency for the overall survival of the displacement in forming a loop is 20%. This loop size is on the order of 120 Å average diameter for irradiation with 20-MeV protons and the displacement model. Calculating displacements with the threshold model results in an average loop size of 65 Å for a 20% overall survival of displacements in the loop. These loop sizes are calculated for perfect circles. Irregularities in the loop boundary would result in larger overall dimensions for the same number of enclosed defects.

The number and size of visible defects has been observed in transmission electron microscopy (TEM) on Cu irradiated at room temperature by 16-MeV protons.[26] The number distribution of defects has an e^{-R/R_0} dependence on radius with $R_0 \sim 20$–25 Å. Using the R_0 value for the average loop radius, the survival fraction of displacements fixed in the loop can be determined for each model. This fraction is 0.04 for the displacement model and 0.07 for the threshold model values in Table I for the high-energy-proton irradiation. Thus, for the defects to be dislocations as determined in Ref. 25 either the displacement survival efficiency is considerably less than 0.20, or the average loop size much greater than ~20 Å observed in Ref. 26.

The validity of the models for calculating displacements can be examined by comparing the model prediction to measured effect as a function of proton irradiation energy. Two predictions of the defect-production energy dependence are plotted with the data in Fig. 5. The predictions are normalized to the trapping rate measured for the 20.5-MeV irradiation in each case. The data show that the displacement model does not describe the energy dependence of the surviving defect concentration observed in this experiment. The calculated rise in damage production at lower proton irradiation energies is not obtained. The calculated increase in the damage production rate for irradiations with lower-energy protons is mainly due to the increased probability of small-angle Coulomb scattering for protons at these energies. If defects which are produced with higher-energy recoils are more stable, then the disagreement between the calculation and experiment can be explained. The threshold model which includes only the effects of high-energy recoils, is shown. This model is obtained by setting a cut-

off in the recoil spectrum at some energy and then calculating damage with the displacement model for all recoils above that cutoff. The value of the cutoff is determined by requiring that the ratio of the damage rates in the high-energy irradiation and the low-energy irradiation be the same in the calculation and the experiment. The value of the threshold when determined in this matter is 55 keV. Plotted with the calculations for the 55-keV threshold are calculations with the threshold model for threshold value of 20 and 100 keV. Recoils in this energy range can produce cascades which result individually in surviving clusters observable in TEM, while recoils with energies much below this energy range do not produce the dynamic clustering seen in TEM. Calculation of the relative defect production with the threshold model gives a good description of the energy dependence observed in the trapping rates. The general trends in the energy dependence of the data are matched reasonably well by calculations with any of the thresholds presented. The threshold at 55 keV clearly gives the best description of the data. The dip at about 10 MeV is matched. This threshold model cannot be entirely correct. There are surviving defects resulting from recoil events below the threshold as demonstrated in reactor-neutron and also electron-irradiation experiments.[4,16-18] The threshold model does demonstrate the relative importance of the high-energy recoils in the room-temperature range.

The discrepancy between the displacement-model predictions and the measured values for the trapping rates is the same magnitude as that obtained in tensile-test comparisons of copper specimens irradiated by either fission neutrons in a reactor or D-T fusion neutrons from the RTNS.[4] Although there has been no demonstration of correspondence between the number of trapping sites and the mechanical parameter of yield strength, the general effect of an increased efficiency for production of surviving defects in more energetic irradiations is the same in both experiments. The reactor-neutron recoil spectrum contained few high-energy recoils ($E > 100$ keV) while the recoil D-T neutron spectrum, because of fusion neutrons, contains a majority of recoils in the energetic region. This resulted in few visible clusters in TEM photographs of the reactor-irradiated samples and easily visible clusters in the fusion-irradiated samples. Thus there is a difference in character of the damage observed in low- versus high-energy recoil production. In the proton experiment, the energy distribution of recoils has a significant fraction above 100-keV energy. Thus, even in the lowest-energy samples tested in this experiment there will be direct production of cascades during the irradiation.

The fission-neutron data prove that subcascade defects survive in copper at these temperatures. Other data suggest that subcascade defects will actually group together to produce new defect structure when produced at low temperature and annealed at near room temperature. This was observed in isochronal-annealing studies of the positron line-shape parameter, positron lifetime, and electrical resistivity of electron irradiated copper.[16,25,26] During annealing stage III in copper, the rate of change in the resistivity of the sample becomes much smaller above $-10\,^{\circ}C$. It is at this stage that the line-shape parameter begins to increase and the trapped positron lifetime changed. The interpretation of these data is that during that stage, the single vacancies are becoming mobile and condensing into stable clusters.

It would appear that there can be two mechanisms for producing surviving defects in energetic irradiations at room temperature and above; direct production of stable structures in the cascade, and the annealing of individual point defects into more stable configurations. The relative effect of these two possible processes can be investigated by an additional data set.

If the defects produced by lower-energy recoils are less stable and can anneal at the temperature ($-4\,^{\circ}C$) at which the majority of the samples were irradiated, then this annealing would be restricted if the samples were irradiated at a sufficiently lower temperature. This would result in a higher concentration of defects at the beginning of the post irradiation anneal at room temperature. Isochronal annealing studies of electron-irradiated copper have shown that some point defects which exist at temperatures below $-10\,^{\circ}C$ will condense upon annealing at room temperature and produce positron traps. This suggests that there should be a higher trapping rate observed for those samples which were irradiated at a temperature below $-10\,^{\circ}C$ and then annealed at room temperature than for those irradiated above $-10\,^{\circ}C$ and then similarly treated.

The samples irradiated at lower temperatures have trapping rates higher than those irradiated at higher temperatures. The trapping rate resulting from the lowest temperature irradiation is enhanced by about a factor of 2.5 over those rates from samples irradiated above $0\,^{\circ}C$. Of special interest, the ratio of the trapping rate at low and high irradiation energies changes as a function of temperature. The values for the samples irradiated at 4.5 and 20.5 MeV are comparable for the irradiation at $-37\,^{\circ}C$ with the 4.5-MeV rate slightly higher. At higher temperatures,

the value for the high-energy irradiation is greater than the low-energy irradiation by as much as $\frac{3}{2}$. This behavior is consistent with the assumption that there are defects frozen in at the lower irradiation temperature which then may cluster into more stable defects at room temperature, and that these defects are produced in greater quantities by lower-energy PKA events. That the defect concentration has two components, one of which need not be frozen until the room temperature anneal, is seen by the fact that there is only a slight decrease in the trapping rate as the irradiation temperature increases from 0 °C to room temperature. The annealing curves both support the assumption that there is only one defect configuration in both energy irradiations and that the defect type is stable at room temperature. The temperature at which the annealing of the traps occurs is typical of both dislocations and vacancy clusters so there is no distinct differentiation of defect type available in the annealing data. Insimilar studies on copper irradiated with reactor neutrons and probed by the Doppler broadening of the positron annihilation radiation, there has been an increase in the fraction of positrons trapped as inferred from the line-shape parameter as the annealing temperature reached 350 °C.[12] No such increase was observed in this experiment. The reason for this is not known. However, the analysis of the neutron-irradiation experiment suggested that the defect produced was dislocation loops rather than the vacancy clusters seen in the present experiment.

VI. SUMMARY

Copper samples have been irradiated with protons at an initial energy of 24 MeV. The samples were stacked so the energy was degraded to 4.5 MeV at the back side of the samples. The sample temperature during irradiation for all runs excepting those used to investigate temperature dependence was −4 °C. The resulting defect concentration and structure was probed by the positron lifetime measurement. The same defect structure was produced in all energy proton irradiations as evidenced by the same value of saturated lifetime for those samples. The dependence of the trapping rate obtained from a single-trap model on proton dose was linear to a high degree over the dose range 0 to 2×10^{17} p/cm^2. There was no evidence for more than one trap in any of the samples, indicating only one defect type was present. The value of the saturated lifetime and the survival efficiency values indicate that the defect type is vacancylike for all measurements.

The dependence of the defect-production rate on proton-irradiation energy was measured and it was found that the energy dependence was not described by the displacement model. A model which did describe the energy dependence more accurately included damage produced by only those copper recoils with energies of more than 55 keV. The description of the damage in the samples as resulting from two processes, one in a low-energy recoil region, the other in a higher-energy region, was demonstrated by lowering the temperature of irradiation so the defects produced by the lower-energy recoils would be kept at a higher concentration during irradiation and would condense to stable defects during the postirradiation anneal. The defect concentration measured was enhanced by a factor of 2.5 by this technique. It was found in isochronal-annealing studies the defects doing the trapping were stable at room temperature, and there is no change in defect character up to the temperature at which the defects are annealed.

ACKNOWLEDGMENTS

The author gratefully acknowledges M. Guinan, J. Mitchell, and C. Logan for their many helpful conversations during the course of this work and C. Poppe for his careful reading of this paper. Work performed under the auspices of the Department of Energy under Contract No. W-7405-Eng-48.

[1]K. L. Merkle, R. S. Averback, and R. Benedek, Phys. Rev. Lett. 38, 424 (1977).
[2]J. B. Roberto, C. E. Klabunde, J. M. Williams, R. R. Coltman, M. J. Saltmarsh, and C. B. Fulmer, Appl. Phys. Lett. 30, 509 (1977).
[3]M. W. Guinan and C. E. Violet, *Symposium on Neutrons 10–40 MeV*, BNL-NCS 506 81 (NTIS, Springfield, Va., 1977), p. 361.
[4]J. B. Mitchell D. M. Parkin, R. A. Van Konynenburg, and C. J. Echer, *Radiation Effects and Tritium Technology for Fusion Reactors*, Conference 750989, (NTIS, Springfield, Va., 1975), p. II–172.
[5]C. M. Logan, J. D. Anderson and A. K. Mukherjee, J. Nucl. Mater. 48, 223 (1973).
[6]A. M. Omar, J. E. Robinson and D. A. Thompson, J. Nucl. Mater., 64, 121 (1977).
[7]M. T. Robinson, *Nuclear Fusion Reactors* (Brit. Nucl. Energy Soc., London, 1970), p. 364.
[8]C. M. Logan (private communication).
[9]C. M. Logan and E. W. Russell, LLL report No. UCRL-52093 (NTIS, Springfield, Va., 1976).
[10]D. M. Parkin and A. N. Goland, Radiat. Eff. 28, 31 (1976).
[11]Osamu Sueaka, J. Phys. Soc. Jpn. 36, 464 (1974).

[12]J. D. McGervey and W. Triftshäuser, Phys. Lett. 44, 53 (1973).
[13]P. Hautojarvi and P. Jauho, Acta Polytech. Scand. Phys. 98, 1 (1973).
[14]W. B. Gauster, S. Mantl, T. Schober, and W. Triftshäuser, *Fundamental Aspects of Radiation Damage in Metals*, Conference 751006 (NTIS, Springfield, Va., 1975), p. 1143.
[15]W. B. Gauster and S. R. Dolce, Solid State Commun. 16, 867 (1975).
[16]S. Mantl and W. Trifthauser, *Fundamental Aspects of Radiation Damage in Metals*, Conference 751006 (NTIS, Springfield, Va., 1975), p. 1122
[17]T. Hadnagy, thesis (University of Utah, 1976) (unpublished).
[18]K. Hinode, S. Tanigawa and M. Doyama, Radiat. Eff. 32, 73 (1977).
[19]T. M. Hall, A. N. Goland, and C. L. Snead, Jr., Phys. Rev. B 10, 3062 (1974).
[20]Nuclear Data Group, $A = 207$ (Academic, New York, 1973).
[21]C. Tschalar, Nucl. Instrum Meth. 61, 141 (1968).
[22]M. W. McNaughton, United Kingdom Atomic Energy Authority No. AERE-R7072, (HMSO, London, 1972).
[23]Allen N. Goland, *Fundamental Aspects of Radiation Damage in Metals*, Conference 751006 (NTIS, Springfield, Va., 1975), p. 1107.
[24]K. Hinode, S. Tanigawa, and M. Doyama, J. Phys. Soc. Jpn. 41, 2037 (1976).
[25]B. T. A. McKee, S. Scumoto, A. T. Stewart, and M. J. Stott, Can. S. Phys. 52, 759 (1974).
[26]J. B. Mitchell, C. M. Logan and C.J. Echer, Nucl. Mat. 48, 139 (1973).